Mon. Not. R. Astron. Soc. **357,** 56–68 (2005) doi:10.1111/j.1365-2966.2004.08572.x

Globular clusters as tracers of stellar bimodality in elliptical galaxies: the case of NGC 1399

Juan C. Forte,[1,2]★ Favio Faifer[1,2] and Doug Geisler[3]

[1]*Facultad de Ciencias Astronómicas y Geofísicas, Universidad Nacional de La Plata*
[2]*Consejo Nacional de Investigaciones Científicas y Técnicas, Rep. Argentina*
[3]*Departamento de Física, Universidad de Concepción, Chile*

Accepted 2004 October 27. Received 2004 October 21; in original form 2004 September 6

ABSTRACT

Globular cluster systems (GCSs) frequently show a bimodal distribution of cluster integrated colours. This work explores the arguments to support the idea that the same feature is shared by the diffuse stellar population of the galaxy they are associated with. The particular case of NGC 1399, one of the dominant central galaxies in the Fornax cluster, for which a new B surface brightness profile and $(B - R_{KC})$ colours are presented, is discussed taking advantage of a recently published wide-field study of its GCS. The results show that the galaxy brightness profile and colour gradient, as well as the behaviour of the cumulative globular cluster specific frequency, are compatible with the presence of two dominant stellar populations, associated with the so-called 'blue' and 'red' globular cluster families. These globular families are characterized by different intrinsic specific frequencies (defined in terms of each stellar population): $S_n = 3.3 \pm 0.3$ in the case of the red globulars and $S_n = 14.3 \pm 2.5$ for the blue ones. We stress that this result does not necessarily conflict with recent works that point out a clear difference between the metallicity distribution of (resolved) halo stars and globulars when comparing their number statistics. The region within 0.5 arcmin of the centre shows a deviation from the model profile (in both surface brightness and colour) that may be explained in terms of the presence of a bulge-like high-metallicity component. Otherwise, the model gives an excellent fit up to 12 arcmin (or 66.5 Kpc) from the centre, the galactocentric limit of our blue brightness profile. The inferred specific frequencies imply that, in terms of their associated stellar populations, the formation of the blue globulars took place with an efficiency about six times higher than that corresponding to their red counterparts. The similarity of the spatial distribution of the blue globulars with that inferred for dark matter, as well as with that of the X-ray-emitting hot gas associated with NGC 1399, is emphasized. The impact of a relatively inconspicuous low-metallicity population, that shares the properties of the blue globulars, as a possible source of chemical enrichment early in the formation history of the galaxy is also briefly discussed.

Key words: galaxies: clusters: individual: NGC 1399 – galaxies: haloes – galaxies: star clusters.

1 INTRODUCTION

A large volume of arguments supports the idea that the current structure of most galaxies has been determined by events that occurred at the very early epochs of the Universe (see, for example, Baugh et al. 1998, and references therein). In this context, and being the oldest stellar systems for which a reliable chronology exists [at least in the Milky Way (MW)], globular clusters (GCs) have become the subject of an increasing amount of research that aims at identifying the link between their formation and that of their host galaxies themselves.

Even though the fact that GCs may be used as probes of the formation of a galaxy has been known for a long time (e.g. Eggen, Lynden Bell & Sandage 1962) and that the knowledge of GC systems (GCS), in our and in other galaxies, has been steadily growing, a unified picture that explains both the small-scale phenomena that lead to the cluster formation and also their overall properties as systems, is still missing.

Recent reviews give good summaries of the situation (e.g. Harris 2003; Kissler-Patig 2002) and compare the features of several astrophysical scenarios that invoke 'external' or 'internal'

★E-mail: forte@fcaglp.unlp.edu.ar

phenomena that provide a reasonable confrontation with observations. It seems clear, however, that some aspects of the problem require a cosmological frame as already suggested by Peebles & Dicke (1968). More recently, other attempts assume hierarchical CDM models (Beasley et al. 2002) that appear as a promising approach to further incorporate the effects of different and coexisting (rather than excluding) processes that end up with the formation of a GCS as, for example, the role of GC as a possible source of the re-ionization of the Universe (Ricotti 2002; Santos 2003).

All those scenarios, however, must take into account some relatively well established facts as boundary conditions, namely.

(i) Stellar clusters that fulfill the properties expected for a 'young' GC are currently formed in violent events, such as galaxy mergers, as originally pointed out by Schweizer (1987). These kind of phenomena, on a variety of scales, were probably more frequent during the early phases of galaxy formation.

(ii) GC formation seems connected with major stellar formation events. This fact is well supported by the relatively narrow range of the ratio of the number of GC to galaxy luminosity, as well as by the correlation of cluster formation with high star formation rate (SFR) (Larsen & Richtler 2000). This ratio can be quantified, for example, using the so-called 'specific GC frequency', S_n, following Harris & van der Bergh (1981). We point out that a revision of several archetypical high S_n galaxies have lowered previous estimates of this parameter by half, or even less (e.g. Ostrov, Forte & Geisler 1998; Forte et al. 2002).

(iii) The MW GC metallicity distribution shows a bimodal structure. This feature seems shared by other galaxies that show bimodal colour distributions (e.g. Geisler, Lee & Kim 1996). Although the well-known colour–age–metallicity degeneracy prevents a stronger statement about the significance of the colour distribution, the assumption of very old ages for GCs points to metallicity as the main driver of the colour distribution.

(iv) In the case of NGC 1399, the so-called 'red' GCs exhibit a distinct behaviour, when compared with the 'blue' GCs, both in terms of their spatial distribution and kinematic behaviour (e.g. Richtler et al. 2004; R2004 in what follows).

In this picture, the connection between the GCS and the stellar population in a galaxy is not completely clear. Some differences (Forte, Strom & Strom 1981) and some similarities (Forbes & Forte 2001) have been pointed out over the years. This last paper, in particular, reinforces previous arguments (Forbes, Brodie & Huchra 1997) that suggest a connection between the red GC and the galaxy halo stars based on the similarity of the red GC colours with those observed in the *inner* regions of a galaxy. A significant contribution to the subject has been presented by Harris & Harris (2002) (and references therein) who discuss the characteristics of the resolved stellar population of NGC 5128 and present a comparison with the GC in that galaxy. These authors also discuss a possible connection between GC specific frequency and metallicity.

This paper explores the arguments to support (or reject) the idea that, in the bimodal GCS, the 'diffuse' galaxy stellar population also exhibits a dual nature reflecting the existence of two major stellar populations that share the properties of each GC family and are typified by a given 'intrinsic' S_n, integrated colour and spatial distribution.

We emphasize that this work presents an approach that, in principle, makes no assumptions about the nature of integrated colours (in terms of ages or metallicities) and finally aims at matching the shape of the observed galaxy surface brightness, colour gradient and cumulative S_n (with galactocentric radius) by properly weighting each of the diffuse stellar components. These stellar populations, defined just in colour terms, then might include a range of age and/or metallicity as well as of GC specific frequencies.

NGC 1399, the central galaxy in the Fornax cluster, appears as a good candidate on which to perform this kind of analysis because, as in other luminous ellipticals, its GCS is well populated and can provide statistically significant results. In addition, it is relatively nearby.

A number of papers have dealt with the clearly bimodal GC colour distribution in this galaxy taking advantage of the high metallicity sensitivity of the colour index defined in terms of the C and T_1 bands of the Washington photometric system (Canterna 1976). These early works (Geisler & Forte 1990; Ostrov, Geisler & Forte 1993; Ostrov et al. 1998) have a relatively small areal coverage. In turn, Dirsch et al. (2003) (D2003 hereafter) increased the surveyed area to about 900 arcmin^2 by means of mosaic charge-coupled devices (CCD) observations and determined GC areal density profiles up to a galactocentric radius of about 20 arcmin. These density profiles, and the surface photometry (Johnson's B and Kron–Cousins R filters) presented in this work are the basis of the subsequent analysis. An attempt to disentangle the stellar populations in NGC 1399 was presented in D2003 although, as described later, with a somewhat different approach.

The structure of the paper is a follows: Section 2 describes the result of composing two stellar populations and the variables that govern the shape of the galaxy surface brightness profile as well as the derivation of the intrinsic specific frequencies of each GC population. The characteristics of the GCS system associated with NGC 1399 and a justification of the adopted distance modulus are presented in Section 3. A new blue profile and $(B - R_{\rm KC})$ colours for the galaxy are presented in Section 4. The areal density run with galactocentric radius for both the red and the blue GCs, as well as the derivation of their volumetric density profiles, are discussed in Sections 5 and 6, respectively. Section 7 gives a confrontation of the observations with the properties of the model in terms of the shape of the surface brightness profile, colour gradient and cumulative GC specific frequencies as a function of galactocentric radius. A caveat about the approach is commented on in Section 8. A first approach to the expected metallicity distribution function (MDF) of the galaxy halo stars is described in Section 9. The total stellar mass as well as the GC formation efficiencies are discussed in Section 10. A comparison of the GC spatial distribution with that inferred for dark matter (R2004) and hot gas obtained from X-ray observations are given in Section 11. A discussion of the results and possible implications on the galaxy formation scenario are included in Sections 12 and 13, respectively.

2 A COMPOSITE SURFACE BRIGHTNESS PROFILE

In what follows we assume that both the red and the blue globulars in NGC 1399 have an associated diffuse stellar population characterized by their own intrinsic specific frequencies.

A generalization of the S_n parameter to any photometric band, and in particular, for the B (Johnson's blue) band, leads to a composite luminosity [in $M(B) = -15$ units]

$$L(B) = \frac{N(\mathrm{RGC})}{S_B(\mathrm{RGC})} + \frac{N(\mathrm{BGC})}{S_B(\mathrm{BGC})}. \quad (1)$$

The blue band is chosen, in this case, as we will attempt to match the shape of the B surface brightness profile presented in Section 4. If N(RGC) and N(BGC) are the projected areal densities of the red and

blue GCs, respectively, and $(V - M_V)_o$ is the (interstellar extinction) corrected distance modulus, for any galactocentric radius

$$(V - M_V)_o = \mu_B - A(B) - M(B), \quad (2)$$

where μ_B is the galaxy surface brightness, $A(B)$ is the interstellar extinction along the line of sight in the blue band, and $M(B) = -2.5 \log(L(B) \times 10^6)$ is the areal absolute blue magnitude, if $L(B)$ is given in absolute brightness units of $M(B) = -15.0$; and if both intrinsic specific frequencies are assumed to remain constant with galactocentric radius, then it follows:

$$\mu_B = (V - M_V)_o + A(B) + 2.5 \log[S_B(\mathrm{RGC})] - 2.5 \log \left[N(\mathrm{RGC}) + \frac{N(\mathrm{BGC})}{C(B)} \right], \quad (3)$$

where $C(B)$ is the ratio of the specific frequencies of the blue to red GC populations, $S_B(\mathrm{BGC})/S_B(\mathrm{RGC})$.

The expression for μ_B shows that, if the areal densities of both cluster families as a function of the galactocentric radius are determined from observations, the shape of the surface brightness profile will depend only on the $C(B)$ parameter.

Aiming at obtaining the best fit to the observed μ_B in terms of the globular specific frequencies we then proceeded in two steps. First, we looked for the $C(B)$ parameter that makes the quantity $\mu_B + 2.5 \log [N(\mathrm{RGC}) + N(\mathrm{BGC})/C(B)]$ constant with the galactocentric radius and, from this constant, after adopting a given distance modulus and interstellar reddening, we obtain $S_B(\mathrm{RGC})$. In turn, $S_B(\mathrm{BGC})$ comes from $C(B)$ and this last parameter.

This procedure differs from that given in D2003 in the sense that: (a) only the profile shape is fitted (colour gradients are predicted and then compared with observations); (b) constant intrinsic specific GC frequencies are assumed (i.e. not forcing a particular functional dependence with galactocentric radius); (c) the derived surface brightness is confronted with an observed profile that relies on genuine sky brightness measurements (as opposed to the adoption of a preferred value as in D2003).

In the following sections we describe all the terms involved in the μ_B expression that will be used to fit the observed blue profile.

3 THE NGC 1399 GLOBULAR CLUSTER SYSTEM AND ITS DISTANCE MODULUS

3.1 Bimodality

The possible existence of a bimodal $(C - T_1)$ colour distribution in the NGC 1399 GCS was suggested by Ostrov et al. (1993) and confirmed in Ostrov et al. (1998) by means of $(C - T_1)$ versus $(M - T_1)$ two colour diagrams. This last work noted that, except in the very inner regions of the galaxy, the modal colours of both cluster families remained at constant values independent of the galactocentric radius. This feature was also noticed by D2003 who extended the survey to about 20 arcmin in radius. As noted in this last work, and based on Geisler (1996), the T_1 and R_{KC} bands are practically identical and in what follows we adopt $(C - T_1)$ as being equivalent to $(C - R_{KC})$.

Fig. 1 shows the $(C - T_1)$ colour distribution for a sample of 1246 GC candidates contained within an annular region between 2 and 7 arcmin of the galaxy centre, taken from the Forte et al. (2002) and D2003 data. The annular boundaries of this region were chosen in order to maximize the number of GC while keeping a low contribution from field interlopers. In turn, the magnitude range covers from $T_1 = 21.0$, to the position of the GC luminosity function

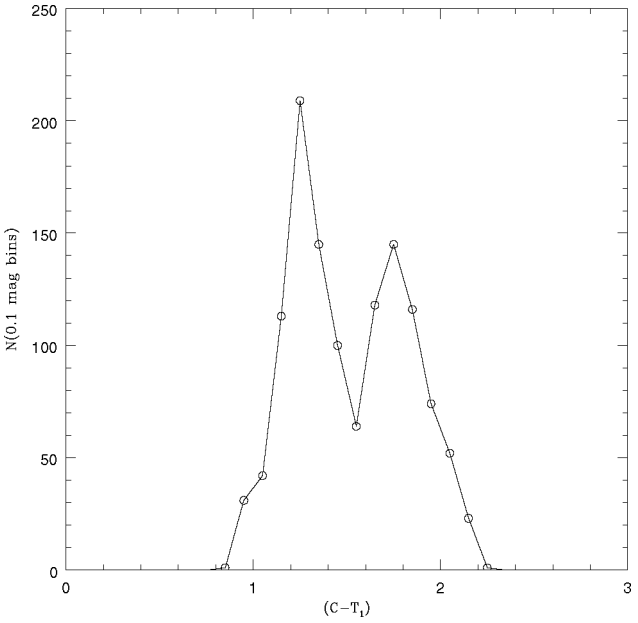

Figure 1. $(C - T_1)$ colour distribution for 1246 GC candidates associated with NGC 1399 and within a galactocentric radii of 2.0–7.0 arcmin. The sample includes globular candidates with T_1 (or R_{KC}) magnitudes between 21.0 and 23.2; colour bins are 0.1-mag wide. Two well-defined modal colours are seen at $(C - T_1) = 1.28$ and 1.77.

turnover at $T_1 = 23.2$. We adopt this value as a compromise between those derived by Geisler & Forte (1990) and Ostrov et al. (1998).

GC candidates brighter than $T_1 = 21$, that were left out of the analysis, constitute a small fraction of the whole cluster population (less than 9 per cent) and their nature remains to be clarified as they exhibit a unimodal colour distribution (noted both in Ostrov et al. 1998, and D2003) and a higher radial velocity dispersion than that characterizing their fainter counterparts (from R2004 data).

A convolution of the original data, that in Fig. 1 appear binned in 0.10-mag intervals, with a Gaussian kernel with a dispersion of 0.05 mag (similar to the photometric errors) leads to $(C - T_1)$ modal colours of 1.28 and 1.77 for the blue and red globulars, respectively. In what follows, and consistent with D2003, we adopt a $(C - T_1)$ colour of 1.55 as a formal boundary between the blue and red GCs (their associated diffuse stellar populations will also be referenced as 'blue' and 'red' in what follows). The colour excess maps by Schlegel, Finkbeiner & Davis (1998) give $E(B - V) = 0.015$ that translates to $E(C - T_1) = 0.030$ along the line of sight to NGC 1399. The resulting intrinsic colours are $(C - T_1)_o = 1.25$ for the blue GC and $(C - T_1)_o = 1.74$ for the red GC. To derive a $(B - R)$ colour gradient and the specific frequencies of both cluster families in the V band, S_n, by means of the best profile fitting to the observed μ_B (Section 5), we used the following transformations:

$$(B - V)_o = 0.508(C - T_1)_o + 0.064 \quad (4)$$

$$(B - R)_o = 0.704(C - T_1)_o + 0.269. \quad (5)$$

These last relations were obtained by means of bisector fits to the intrinsic colours of MW globulars (Reed, Hesser & Shawl 1988) that also give a good representation of intrinsic colours in galaxies with redder globulars (see Forbes & Forte 2001) and yield $(B - V)_o = 0.68$, $(B - R)_o = 1.13$ for the blue GC and $(B - V)_o = 0.95$, $(B - R)_o = 1.49$ for the red GG with an overall uncertainty of $\approx \pm 0.03$ mag.

3.2 Distance modulus

We derive a distance modulus to NGC 1399 by means of the turnover magnitude of the blue GC, $B_{to} = 24.32$ mag, obtained by Grillmair et al. (1999) on the basis of their *Hubble Space Telescope* (*HST*) photometry. In order to avoid corrections for metallicity effects (e.g Ashman, Conti & Zepf 1995) we compare that magnitude with the mean blue absolute magnitude of MW globulars with $(C - T_1)_o$ colours in the same range. The Harris (1996) compilation includes 35 globulars with a mean $(C - T_1)_o = 1.15$ (i.e. slightly bluer than the N1399 mean blue GC colours) and a mean absolute magnitude $M(B) = -7.15 \pm 0.3$. Adopting $A(B) = 0.06$ mag [consistent with the $E(B - V)$ excess mentioned above] leads to $(V - M_V)_o = 31.4$ (corresponding to 19 Mpc). This distance modulus agrees with that adopted by R2004 who give a summary of other distance estimates available in the literature.

4 BLUE SURFACE BRIGHTNESS PROFILE AND $(B - R_{KC})$ COLOURS FOR NGC 1399

The determination of galaxy surface brightness profiles over large galactocentric radii faces well-known problems connected with the adoption of a proper sky level and flat fielding (particularly severe in wide-field instruments). Small-field telescopes, on the other hand, are more manageable in terms of flat-field quality but, in the case of objects with large angular sizes, do not allow the measurement of a meaningful sky brightness.

In this work we used the 2.15-m telescope at the Complejo Astronómico El Leoncito (San Juan, Argentina) in combination with a focal reducer that gives an effective field of 9 arcmin on the CCD detector. Simultaneous and continuous measurements of the sky brightness were obtained by means of a zenithal airglow sensor (Scheer 1987) that measures the intensity of atmospheric molecular emission lines. These measurements were correlated with B and R_{KC} sky brightness estimates made on CCD frames taken 40 arcmin to the north of the galaxy centre (and intertwined with the galaxy field images).

The correlation took into account the differences in airmass between the zenith and the line of sight to the galaxy as well as atmospheric extinction (derived during the run: $k_B = 0.29$; $k_R = 0.08$). The sky brightness to be subtracted from each galaxy field was then obtained by interpolating its temporal behaviour derived from the airglow versus sky frames correlation.

Sky flats were obtained immediately after sunset and provided an overall flat-field on the order of 0.5 per cent.

The observation sequence included sets of four images (15 min exposures) centred on the galaxy and off set frames taken along a position angle of 45° (north to east) and reaching a galactocentric distance of about 12 arcmin. This direction is clean of bright galaxies that may contaminate the NGC 1399 outer profile.

Typically, the B sky magnitude ranged from 23.1 to 23.3 mag arcsec^{-2} during the night. We note that the observing run took place in 1997 December and during a period of exceptionally low airglow level coincident with a minimum of solar activity.

Images centred on the galaxy were processed with the ELLIPSE routine within IRAF[1] and delivered brightness profiles that reach 240 arcsec from the galaxy centre. The blue profile was extended up to 510 arcsec using three 20-min exposure images obtained with the 4-m Blanco Telescope at CTIO (described in Forte et al. 2002). These last images are not suitable for an estimate of the sky level and where then matched to our own profiles by means of the method described by Caon, Capaccioli & Donofrio (1994).

The much higher sky brightness in the R_{KC} band prevented a similar approach, restricting the limiting galactocentric radius to 240 arcsec with a maximum estimated error of ±0.04 mag at that radius.

In the case of the off-centre blue frames, aperture photometry was carried out within 25 square windows (5 arcsec per side) located on a region of the images where the flat-field was considered better than 0.2 per cent and far from bright stars (to avoid any spurious scattered light). These measures provide the surface brightness at mean galactocentric radii of 410, 470 (overlapped with the extended profile), 605 and 730 arcsec.

The final composite blue profile is shown in Fig. 2 and listed in Table 1 where $(B - R_{KC})$ colour indices are also given up to an elliptical galactocentric radius of 228.8 arcsec. The elliptical galactocentric radius ($r_e = \sqrt{ab}$) was computed using the ellipticities delivered by ELLIPSE and adopting a constant ellipticity $\epsilon = (1 - b/a) = 0.13$ for the two outermost off-set frames. Error bars depict the error of the mean magnitude derived on the outer CCD frames.

Fig. 2 also includes, as a reference, the fit of a Sérsic law, $\mu_B = b_0 + b_1(r_e/\alpha)^n$, with $b_0 = 3.74$, $b_1 = 1.086$, $\alpha = 4.82 \times 10^{-13}$ and $n = 0.0878$.

Large-field blue surface brightness profiles for NGC 1399 have been published by Killeen & Bicknell (1988) (who combine their observations with V values from Schombert 1986) and by Caon et al. (1994). A comparison between these profiles shows marked differences that increase with galactocentric radius. Fig. 3 shows the brightness residuals as a function of $r_e^{1/4}$ when comparing the profiles of those authors with ours (that, approximately, falls in the middle of both). This diagram also includes a comparison with the

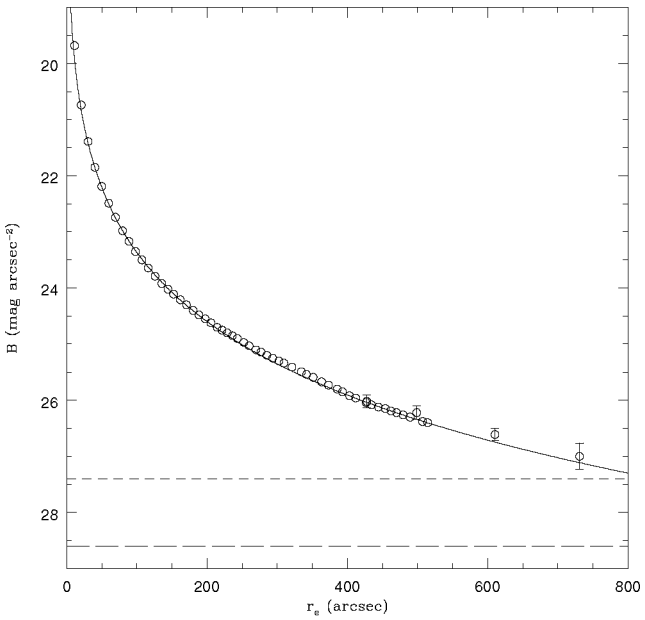

Figure 2. Blue surface brightness profile for NGC 1399 as a function of elliptical radius ($r_e = \sqrt{ab}$). The bars correspond to the error of the mean magnitude. Errors for galactocentric radii smaller than 400 arcsec are comparable to the size of the plotted symbols (± 0.03 mag.) The solid line is a Sérsic profile. The long dashed and short dashed lines correspond to 1σ and to 3σ uncertainties of the sky level.

[1] IRAF is distributed by National Optical Astronomy Observatories, which are operated by the Association of Universities for Research in Astronomy, Inc., under co-operative agreement with the National Science Foundation.

Table 1. NGC 1399 surface brightness photometry.

r (arcsec)	$\log r$	$r^{1/4}$	B	$B-R_{KC}$
11.20	1.049	1.829	19.68	1.58
20.80	1.318	2.136	20.74	1.53
30.50	1.484	2.350	21.39	1.51
40.10	1.603	2.516	21.85	1.50
49.80	1.697	2.656	22.19	1.49
59.80	1.777	2.781	22.49	1.51
69.60	1.843	2.888	22.74	1.49
79.70	1.901	2.988	22.98	1.48
88.80	1.948	3.070	23.17	1.48
98.20	1.992	3.148	23.35	1.46
107.30	2.031	3.218	23.50	1.47
116.10	2.065	3.283	23.64	1.47
125.80	2.100	3.349	23.79	1.46
135.50	2.132	3.412	23.92	1.47
144.20	2.159	3.465	24.02	1.45
152.30	2.183	3.513	24.11	1.45
161.90	2.209	3.567	24.21	1.43
170.60	2.232	3.614	24.30	1.44
180.20	2.256	3.664	24.40	1.44
188.70	2.276	3.706	24.48	1.41
197.40	2.295	3.748	24.55	1.41
205.60	2.313	3.787	24.62	1.41
214.30	2.331	3.826	24.70	1.40
221.40	2.345	3.857	24.75	1.40
228.80	2.359	3.889	24.80	1.41
236.20	2.373	3.920	24.85	
243.20	2.386	3.949	24.90	
252.20	2.402	3.985	24.97	
260.00	2.415	4.016	25.03	
269.60	2.431	4.052	25.10	
276.80	2.442	4.079	25.14	
285.30	2.455	4.110	25.20	
293.50	2.468	4.139	25.25	
302.70	2.481	4.171	25.30	
309.60	2.491	4.195	25.34	
321.10	2.507	4.233	25.41	
334.40	2.524	4.276	25.49	
341.70	2.534	4.299	25.54	
351.30	2.546	4.329	25.59	
363.30	2.560	4.366	25.67	
373.00	2.572	4.395	25.73	
385.40	2.586	4.431	25.80	
393.10	2.595	4.453	25.85	
403.00	2.605	4.480	25.92	
411.80	2.615	4.505	25.96	
426.80	2.630	4.545	26.04	
427.80	2.631	4.548	26.02(±0.11)	
434.50	2.638	4.566	26.08	
444.30	2.648	4.591	26.12	
454.00	2.657	4.616	26.15	
462.00	2.665	4.636	26.19	
470.00	2.672	4.656	26.22	
479.40	2.681	4.679	26.26	
489.50	2.690	4.704	26.30	
498.90	2.698	4.726	26.22(±0.12)	
507.10	2.705	4.745	26.38	
514.60	2.711	4.763	26.40	
610.50	2.786	4.971	26.61(±0.11)	
731.00	2.864	5.200	27.00(±0.23)	

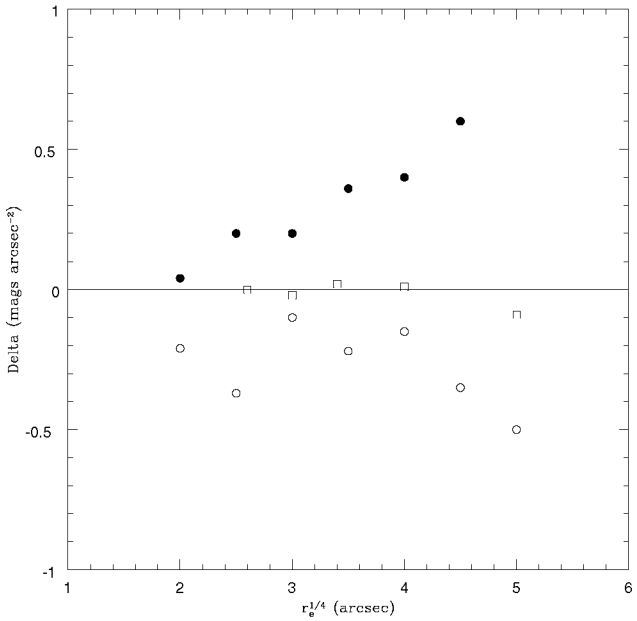

Figure 3. Comparison between the blue profile presented in this work with that given by Killeen & Bicknell (1988) (open circles), Caon et al. (1994) (filled circles) and Hilker et al. (1999) (squares). The V profile of Hilker et al. (1999) was transformed adopting a constant of $(B-V)=0.93$.

V brightness profile presented by Hilker, Infante & Richtler (1999), by adopting a constant difference $(B-V)=0.93$, indicating a good overall agreement (although some residual differences might be expected if a colour gradient were present).

D2003 present R_{KC} and C profiles that reach some 20 arcmin in galactocentric radius. These profiles were obtained by adopting a preferred sky brightness on the basis of measurements at the edge of the images. In particular, their R_{KC} profile is referred to again in Section 7.

5 THE AREAL DENSITY PROFILES

Numerous studies of GCS in luminous elliptical galaxies agree in the sense that the behaviour of the areal densities of the the blue and red GC show a similar behaviour from galaxy to galaxy: blue clusters usually show a more shallow distribution than that corresponding to the red ones which, in turn, show density slopes more similar (but not always identical) to that of the galaxy haloes. A custommary approach uses $r^{1/4}$ laws to fit the density run with galactocentric radius although these approximations fail in the inner regions where GCS exhibit flat cores (see for example, Kundu & Whitmore 1998; Lee, Lee & Gibson 2002). These core profiles show a marked difference with the galaxy light profiles. This last feature has been used to estimate the rate of GC destruction owing to gravitational effects in NGC 1399 and in other galaxies (Capuzzo-Dolcetta & Tesseri 1999; Capuzzo-Dolcetta & Donnarumma 2001).

Fig. 4 depicts the areal density of the red GC derived from D2003 data. An attempt to derive the ellipticity of the red clusters distribution (and also for the blue ones) based on azimuthal counts, indicates a value close to zero (comparable with that of the galaxy itself), which we adopted in what follows. The inner values (filled circles) were derived from *HST* observations given by Forbes, Brodie & Grillmair (1998). Their counts were normalized to a limiting magnitude $T_1=23.2$ and scaled down by 2/3. This last factor takes into

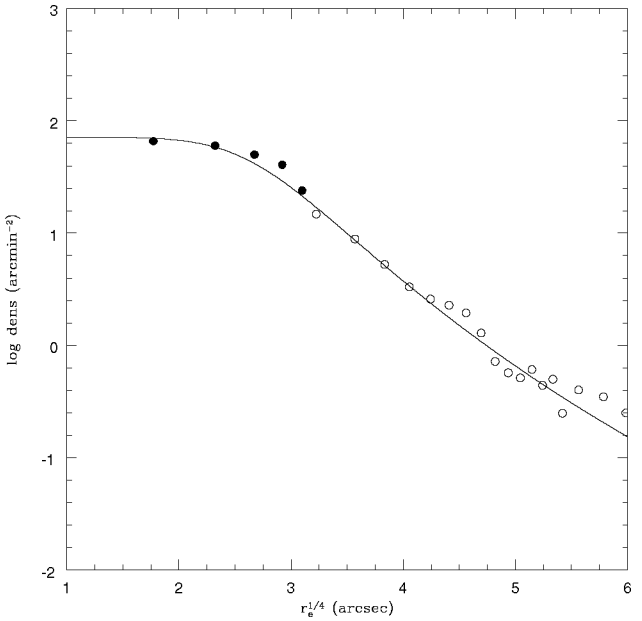

Figure 4. Areal density of the NGC 1399 red GCs. Open circles from data of Dirsch et al. (2003). Filled circles from the (scaled) density profile given by Forbes et al. (1998). The solid line is the approximate fit of a Hubble law with $r_c = 60$ arcsec and a central density of 72 globulars per arcmin^2 (down to magnitude $R = 23.2$).

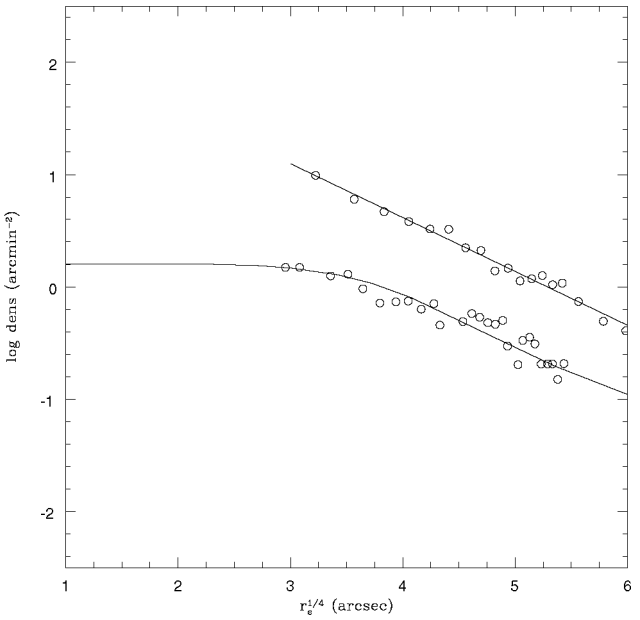

Figure 5. Areal density of the NGC 1399 blue GCs. The straight line is the best formal fitting with an $r^{1/4}$ law. The lower set of values corresponds to the bluest globulars (see text) fit with an isothermal profile with a core radius of 275 arcsec.

account that only this fraction of the GC seem to belong to the red population on the basis of the colour statistics in the inner region of the galaxy, also based on *HST* observations, presented by Grillmair et al. (1999).

For comparison purposes only, Fig. 4 also shows a Hubble law characterized by a central density of 72 GC arcmin^{-2} and a core radius of 60 arcsec.

The blue GC density profile is depicted in Fig. 5 that also includes the best formal fitting with an $r^{1/4}$ law. In this case we note that there is a marginal trend in the sense that the bluest clusters($(C - T_1) = 0.90$ to 1.20, also shown in the same figure) exhibit a shallower core. As a reference we tentatively fit an isothermal profile (Binney & Tremaine 1987) with a core radius of 275 arcsec for these objects. However, this feature will require further confirmation using a deeper sampling and, in what follows, we consider the blue GC as a single family.

One important aspect related with the determination of the GC density profiles at large galactocenric radii is the impact of unresolved field interlopers with colours similar to those of the clusters. We stress that D2003 data were processed with a highly successful procedure for the identification of non-resolved sources, as the GCs are expected to be at the Fornax cluster distance. Further spectroscopic data presented in R2004 indicate a contamination level of the order of 10 per cent or less. In addition, their comparison field (30 arcmin per side) located 3° towards the NE of NGC 1399, provides a very solid estimate of the background level in terms of the uncertainties of the statistical counts (see Section 7).

6 THE GLOBULAR CLUSTER VOLUMETRIC DENSITY PROFILES

Volumetric density profiles allow an estimate of the total mass within a given spatial galactocentric radius as well as a comparison with other galaxy components (e.g. hot gas, dark matter) and, also, to estimate the effect of an eventual (spatial) colour gradient on the projected integrated colours. We note that neither the galaxy light profile nor the GC areal densities can be approximated by means of single (spatial) power laws (r^{α}) except for limited ranges in the galactocentric radius. In this work, and following R2004, we adopt integrable volumetric density functions of the form

$$\mathrm{Dens}(r) = \rho_{\mathrm{o}} \left(\frac{r_{\mathrm{s}}}{r}\right)^{\zeta} \left(\frac{1}{1 + r/r_{\mathrm{s}}}\right)^{3-\zeta} \qquad (6)$$

and aim to determine the ζ and r_{s} parameters that, once Dens(r) is integrated along the line of sight, give a good representation of the projected (or areal) density profiles. The integration was carried out within a limiting radius equal to the virial radius derived by R2004, $R_{\mathrm{vir}} \approx 5800$ arcsec. We note, however, that changing this limit by a considerable amount does not have a large effect on the results of the integration.

The best formal fits to the areal density of the red GC are displayed in Fig. 6. The results show that different combinations of the $\zeta - r_{\mathrm{s}}$ parameters can yield almost equivalent fits within the range of the fit (120–1200 arcsec) and that this degeneracy breaks up only in the innermost regions of the galaxy. However, deciding which of these profiles might be the best representation of the *original* GC distribution is probably impossible as the disrupting gravitational effects are expected to be important in these regions.

Fig. 7 shows the same kind of diagram for the blue GC.

7 RESULTS

This section presents the results of fitting the composite stellar population profile described in Section 3 to the blue surface brightness presented in Section 4. The quality of the fit is estimated in terms of the following.

(1) Shape of the surface brightness profile.
(2) Colour gradient.
(3) Cumulative GC specific frequency.

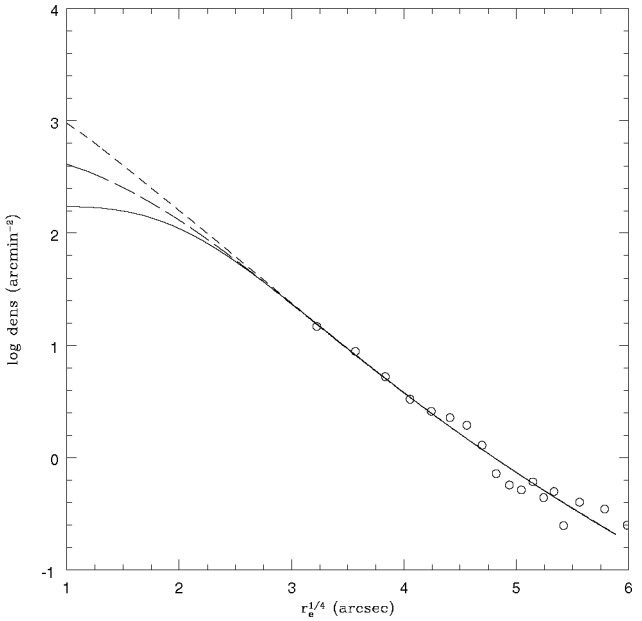

Figure 6. Projected volumetric density profiles that give an adequate fit to the observed red GC surface density (circles) for a given combination of r_s and ζ values (see text); $\zeta = 1.5$, $r_s = 70$ arcsec (short dashed); $\zeta = 1.0$, $r_s = 50$ arcsec (long dashed); $\zeta = 0.0$, $r_s = 30$ arcsec (solid line). The profiles overlap for galactocentric radii larger than 80 arcsec.

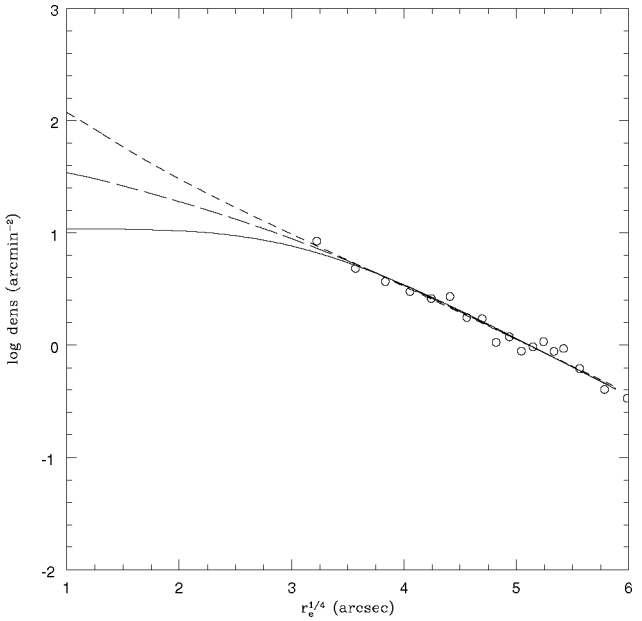

Figure 7. Same as Fig. 6 but for the blue GC (open circles). $\zeta = 0.0$, $r_s = 200$ arcsec (continuous line); $\zeta = 1.0$, $r_s = 400$ arcsec (long dashed); $\zeta = 1.5$, $r_s = 700$ arcsec (short dashed). Profiles overlap for galactocentric radii larger than 150 arcsec.

7.1 The shape of the surface brightness profile

To derive the best fitting to the observed blue surface brightness profile (defined as the one that minimizes the square of the brightness residuals) we proceeded as follows.

(i) A grid of volumetric density profiles that, once projected, provide acceptable fits (with residuals within 1.5 times the mimimum dispersion) to the observed areal densities was generated for each GC family (setting $\zeta = 0.0$, 1.0 and 1.5) and changing the r_s parameter.

(ii) These profiles were projected on the sky (from r = 0 to 1200 arcsec) and then combined within the μ_B equation (described in Section 2). The constant $C(B)$ was iteratively changed until the quantity $k = \mu_B + 2.5 \log [N(\mathrm{RGC}) + N(\mathrm{BGC})/C(B)]$ remained constant with the galactocentric radius, yielding a value of 33.70. The minimum dispersion of this quantity (± 0.035) was obtained by combining GC density profiles characterized by $\zeta = 1.5$ and $r_s = 30$ arcsec for the red GCS, and $\zeta = 1.0$ and $r_s = 375$ arcsec for the blue GC.

(iii) The k value was equated to $(V - M_V)_o + A(B) + 2.5 \log [S_B(\mathrm{RGC})]$ and, by adopting the corrected distance modulus and interstellar extinction discussed in Section 3, the intrinsic specific frequency of the red GC was derived. The specific frequency of the blue clusters follows from $C(B)$ and $S_B(\mathrm{RGC})$.

This procedure leads to $C(B) = 3.5 \pm 0.5$, $S_B(\mathrm{RGC}) = 7.8$, $S_B(\mathrm{BGC}) = 27.3$. The uncertainty for the $C(B)$ parameter comes, mainly, from the range of values allowed by the errors in the outermost region of the brightness profile. The resulting brightness profile is compared with the observations in Fig. 8 and the fit residuals are shown in Fig. 9. This last diagram indicates that, from 30 to 720 arcsec the approach gives a very good fit to the observations with maximum deviations of about ± 0.05 mag and an overall rms of ± 0.035 mag.

The inner 30 arcsec show a deviation in the sense that the nuclear region is brighter than the model. Improving the fit in this region might require a higher ζ exponent (and also the consideration of seeing effects). However, as discussed later, some arguments support the presence of a distinct stellar population in the galaxy nucleus.

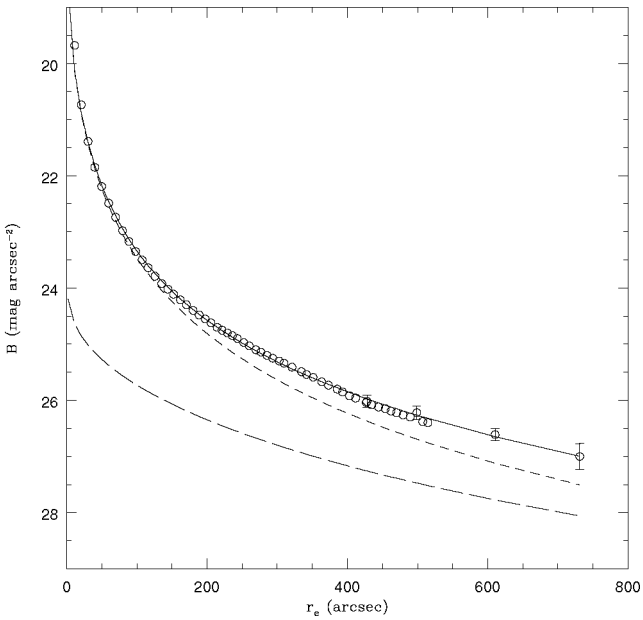

Figure 8. Best profile fit to the observed blue surface brightness of NGC 1399 (solid line). The short dashed line corresponds to the light contribution of the 'red' stellar population; the long dashed line is the light contribution from the 'blue' stellar population. The associated GC have $S_n(\mathrm{RGC}) = 3.3$ and $S_n(\mathrm{BGC}) = 14.3$.

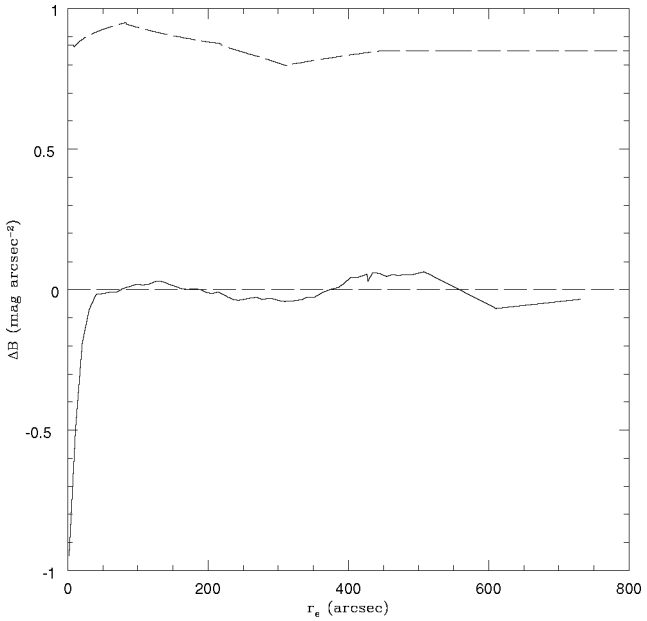

Figure 9. Blue profile fit residuals as a function of the elliptical galactocentric radius r_e (solid line). The maximum deviations are within ± 0.05 mag with an overall rms of ± 0.035 mag over a galactocentric radius from 30 to 730 arcsec. Note the marked deviation within 30 arcsec. The upper (dashed) curve shows the variations of the galaxy flattening ($q = b/a$). A constant q value (0.83) was adopted for r_e larger than 420 arcsec.

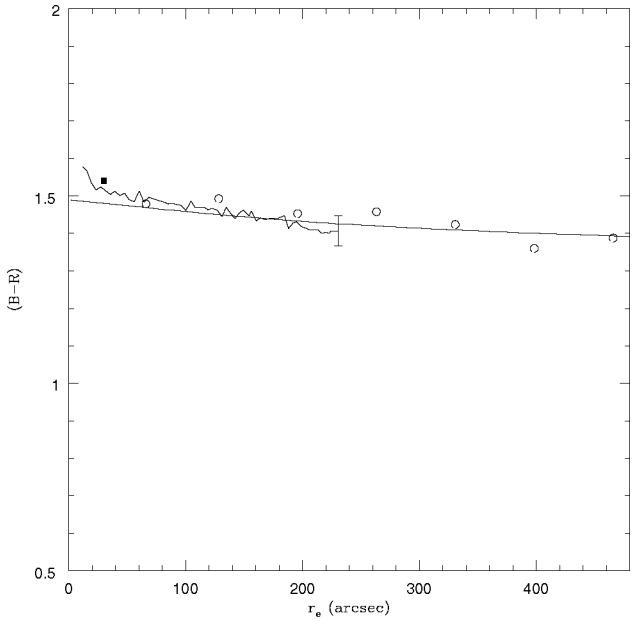

Figure 10. Galaxy $(B - R_{KC})$ colour as a function of elliptical galactocentric radius r_e (solid curve). The straight line is the expected gradient from the model described in Section 2. The square indicates the $(B - R_{KC})$ colour measured by Michard (2000) at $r_0 = 22.8$ arcsec. The bar at 228.8 arcsec indicates the uncertainty of our colour gradient. Open circles show the resulting colour gradient obtained by combining our photometry and that given in D2003 (see text).

The volumetric profiles assumed a spherical geometry. Even though the nature of the residuals in Fig. 9 cannot be completely asserted, we note that they seem correlated with the ellipticity variations depicted in the upper curve of that figure. The assumption of an oblate geometry did not improve the fit suggesting the necessity of a three axis ellipsoid for a further comparison.

We stress that, owing to the small fractional contribution of the blue stellar population to the integrated light in the inner regions of the galaxy, the fit is rather insensitive to the set of $r_s - \zeta$ values adopted for the blue GC. The reason for adopting the quoted values are commented on in Section 11.

7.2 Sources of uncertainty

One source of uncertainty comes from the background level adopted as being representative of the field contamination by non-resolved objects with colours in the domain of the GC colours. The comparison field used by D2003 indicates values of 0.31 and 0.08 objects per arcmin^2 for the blue and red GC, respectively. This field (approx. 35×35 arcmin) includes a large number of objects and yields low counting uncertainties (± 0.016 and ± 0.008). However, the doubt remains in the sense if this is in fact representative of that of the central regions of the Fornax cluster (3° away to the SW).

An increase (decrease) of the background levels by 50 per cent of the adopted values changes the shape of the density (and brightness) profiles forcing an increase (decrease) of the $C(B)$ ratio of ≈ 0.5 in order to keep an acceptable fit to the observed profile.

The combined uncertainty of the quantities involved [k: ± 0.035; $A(B)$: ± 0.02; $(V_o - M_V)$: ± 0.1] lead to ± 0.8 in the S_B(RGC) parameter. This value, and the quoted uncertainty on the $C(B)$ ratio, in turn yield ± 4.8 for S_B(BGC).

7.3 $(B - R_{KC})$ colour gradient

A composite red profile was computed by adding the red light contribution of each stellar population [adopting the $(B - R_{KC})$ colour indices and colour excess discussed in Section 3]. The resulting $(B - R_{KC})$ colour gradient is displayed in Fig. 10, that also includes the observed values listed in Table 1. This diagram shows that, at galactocentric radii larger than 30 arcsec, the predicted colours are consistent with the observations. In turn, these observations are in very good agreement with Michard (2000). This last author gives, at a galactocentric radius $r_0 = 22.8$ arcsec, $(B - R_{KC}) = 1.54$ (0.02 mag redder than ours) and a colour gradient $\mathrm{d}\log(B - R_{KC})/\mathrm{d}\log(r) = -0.05$ that compares well both with the observed (-0.06 ± 0.02) and with the predicted (-0.045) colour gradient.

Another estimate of the $(B - R_{KC})$ gradient was obtained by combining our blue profile and the R_{KC} one given in D2003. These last authors adopted a 'preferred' sky level and warned about the high sensitivity of the profile at the outermost radius. The uncertainty of their profile becomes $\approx \pm 0.05$ mag within a galactocentric radius of 8 arcmin that we adopt as the boundary of our combined $(B - R_{KC})$ colour profile. The resulting $(B - R_{KC})$ is also depicted in Fig. 10 after applying a zero-point shift of -0.1 mag. This correction is necessary to bring the resulting colours into agreement with Michard (2000) and with ours.

As a summary, both our observed $(B - R_{KC})$ gradient and the one derived by combining our blue profile with the red one from D2003, are consistent with the predictions of the profile fit.

7.4 The intrinsic and cumulative GC specific frequencies

The intrinsic specific frequencies derived for each GC family were transformed to the V band, adopting the $(B - V)_o$ colours given

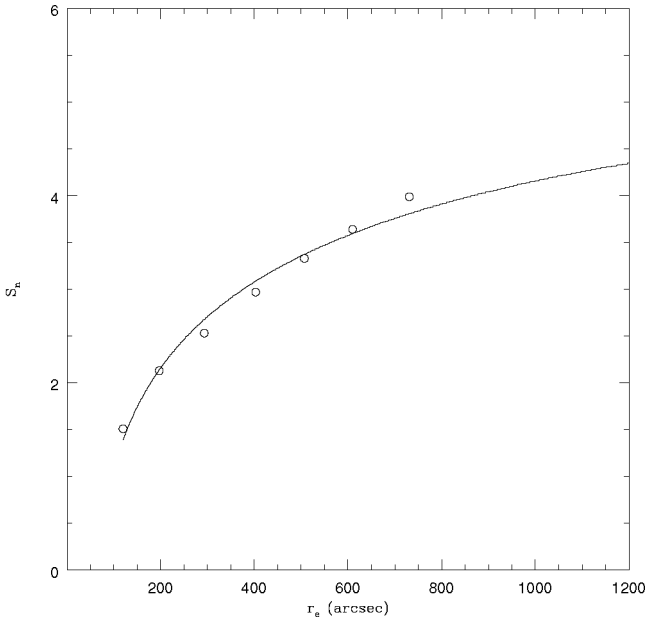

Figure 11. Cumulative specific frequency of the GCS associated with NGC 1399. Open circles represent S_n values derived from the actual counts (transformed to total GC population; see text) combined with the V surface brightness profile predicted by the model. The solid line comes from both the fitted GC areal densities and the model V profile.

in Section 3, yielding S_n(RGC) = 3.3 ± 0.3 and S_n(BGC) = 14.3 ± 2.5. In the case of the red GC, the derived specific frequency is coincident with the representative value quoted for normal ellipticals (see Harris, Harris & McLaughlin 1998). The composite cumulative (with galactocentric radius) specific frequency was computed adopting a total number of 700 GC within a galactocentric radius of 120 arcsec (from the density curve given by Forbes et al. 1998). GC counts at larger radii were derived from D2003 data adopting a limiting magnitude $T_1 = 23.2$, a fully Gaussian integrated luminosity function with a turnover at this magnitude, and an overall completeness of 90 per cent. In turn, the galaxy V surface brightness profile was derived from our observed blue profile and the $(B - V)$ colour gradient computed from the model fit. The adoption of the distance modulus and interstellar extinction discussed in Section 3 lead to the S_n values shown in Fig. 11. The derived cumulative S_n is somewhat smaller, but comparable within the uncertainties, with results given in D2003 and in previous works Ostrov et al. 1998; Forte et al. 2002, that have pointed out that the NGC 1399 GCS cannot be considered as an anomalously high S_n system.

8 A CAVEAT ABOUT THE APPROACH

An alternative fitting to the observed surface brightness profile can be obtained by assuming that the stellar halo follows a density profile similar to that of the red GC and *forcing* a spatial colour gradient $\mathrm{d}(B - R_{\mathrm{KC}})/\mathrm{d}(\log r) = -0.045$.

This blueward trend with increasing galactocentric radius, if owing to a change of metallicity, would increase the B brightness of the stellar population (at constant mass) in the outer regions. The luminosity increase was estimated from Worthey (1994) population synthesis models and assuming an age of 12–17 Gyr (the results are not very sensitive to age in this regime). The forced spatial gradient also provides a good fit to the observed projected $(B - R_{\mathrm{KC}})$ colour gradient.

If that gradient were also shared by the red GC, their (projected on the sky) number versus colour statistic, computed on the basis of the volumetric density profile, would show a modal colour shift of −0.14 mag in $(B - R_{\mathrm{KC}})$, and close to −0.20 mag in $(C - T_1)$, over a galactocentric radius of 20 arcmin. This result is in conflict with the observations (e.g. D2003) that show a practically constant modal colour with galactocentric radius for both GC populations.

Despite this last comment, the main caveat about the profile fit approach presented in this work is the possibility that the chemical enrichment history of the red field stellar population might be decoupled from that of the red GC. In fact there are theoretical reasons to expect some degree of decoupling. For example, if GC form at the beginning of the starburst when external pressure and content of gas is highest; as the SFR decreases, chemical enrichment may continue to occur (but no new GC are formed). This would presumably lead to a colour difference between GC and the galaxy halo. We note, however, that in the case of the halo, the result will be luminosity weighted, i.e. the effect on the colour will depend upon the ratio of the number of stars formed during the SFR peak and those formed subsequently. If this ratio is high, the resulting halo colour could be only slightly redder than those of the RGC.

9 THE STELLAR METALLICITY DISTRIBUTION FUNCTION

This section presents a tentative picture about the expected stellar MDF based on the two-component model presented above. Observations of resolved stars in the halo of NGC 5128 show marked differences of their metallicity distribution when compared with that of GC in number by number statistics (Harris & Harris 2002).

If in fact the GC specific frequency is the result of a composite population, as suggested by the previous section, an estimate of the number ratio of metal-rich (red population) to metal-poor (blue population) stars can be derived through the intrinsic specific frequencies and their mass to light ratios.

The expected stellar mass associated with N clusters within a (projected or spatial) galactocentric radius is $M(\mathrm{stellar}) = (M/L)(N/S_n)$. For the red population we adopt blue $(M/L)_{\mathrm{redpop}} = 10$ derived by Saglia et al. (2000) for the inner regions of NGC 1399 (where that population is dominant) on the basis of their kinematics study. By assuming that the colour difference between both stellar populations arises, mostly, from a metallicity difference close to 1.0 dex (see below), and the results from stellar population modelling (e.g. Worthey 1994), we get $(M/L)_{\mathrm{bluepop}} = 5.75$ for the blue population. This ratio is consistent with the fact that the turnover of the integrated luminosity function of the blue GC in the blue band is about 0.4 mag brighter than that of the red GC as determined by Grillmair et al. (1999).

The resulting stellar mass ratio is then

$$\frac{M(\mathrm{Red})}{M(\mathrm{Blue})} = \frac{S_B(\mathrm{BGC})}{S_B(\mathrm{RGC})} \frac{(M/L)_{\mathrm{redpop}}}{(M/L)_{\mathrm{bluepop}}} \frac{N(\mathrm{RGC})}{N(\mathrm{BGC})} \quad (7)$$

In the particular case of the region between 120 and 420 arcsec of galactocentric radius (see Fig. 1) where $N(\mathrm{RGC}) \approx N(\mathrm{BGC})$, the adoption of the specific frequencies derived in Section 7, leads to a mass ratio close to 6. If the stellar mass distribution function of both populations do not differ markedly, this result implies that blue stars will be relatively inconspicuous in a number statistic that will be largely dominated by the red population stars.

The shape of the MDF for these stars can the be estimated by transforming the GC colours to metallicity and combining both populations according to the mass scaling factor derived above. This procedure deserves a cautious comment taking into account several factors that may have an impact on colour–metallicity relations, like the morphology of the horizontal branch stars (Lee, Lee & Gibson 2002) or the existence of an age spectrum among the NGC 1399 GC (Forbes et al. 2001).

Integrated $(C - T_1)$ colours for the GC sample shown in Fig. 1, that covers a galactocentric radius from 11 to 38 Kpc, were transformed to metallicity by means of the calibration presented by Harris & Harris (2002)

$$[\mathrm{Fe/H}] = -6.037\left[1.0 - 0.82(C - T_1)_o + 0.162(C - T_1)_o^2\right] \quad (8)$$

that improves the linear relation given by Geisler & Forte (1990). The GC sample was divided in two groups: blue GC with $(C - T_1) = 0.9$ to 1.60 and red GC with $(C - T_1) = 1.5$ to 2.2 (i.e. allowing a 0.1-mag overlap between both samples) and correcting for interstellar reddening.

The resulting MDF (in relative units), after applying the scaling factor described before, is shown in Fig. 12. This distribution shows good qualitative agreement with that corresponding to the outer fields in NGC 5128 from Harris & Harris (2002), i.e. a dominant red population with a tail extending to low metallicity values. The results of these last authors stand on colour-magnitude diagrams of resolved stars interpreted in terms of evolutionary tracks with different ages and metallicities. In turn, the MDF presented in this work relies on an empirical integrated colours versus metallicity relation. As a consequence, any further quantitative comparison will require previous effort to check for the consistency of both approaches in terms, for example, of the metallicity scale.

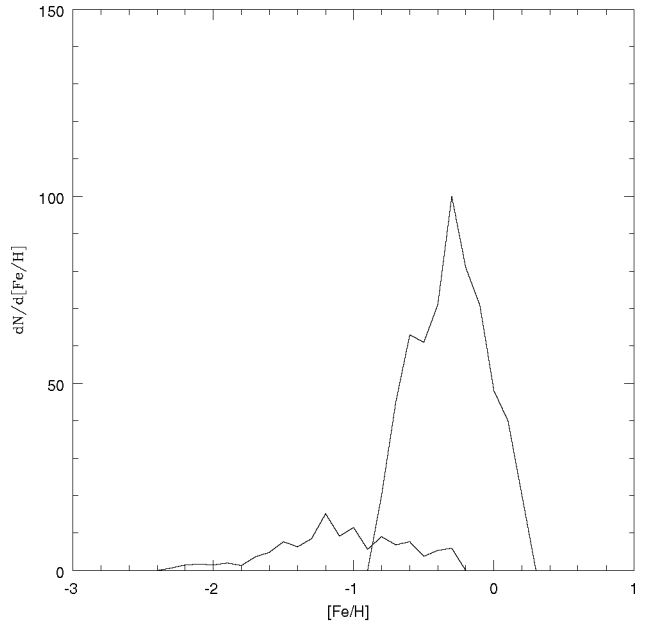

Figure 12. Expected MDF for the stellar population within a (projected) galactocentric radius of 2–7 arcmin whose colour distribution is shown in Fig. 1. The predicted composite MDF shows a good qualitative agreement with observations of resolved halo stars in NGC 5128 (Harris & Harris 2002), i.e. a dominant and wide high-metallicity population and a less conspicuous and extended blue tail.

10 STELLAR MASS AND GLOBULAR CLUSTER FORMATION EFFICIENCY

The GC formation efficiency is a key parameter in understanding the link between these clusters an the diffuse stellar population of the halo. For a given GC specific frequency, the formation efficiency, in terms of the associated stellar mass, is

$$\eta = \frac{S_n(\lambda) M_{\mathrm{GC}}}{(M/L)c}, \quad (9)$$

where (M/L) is the mass to luminosity ratio of the population, M_{GC} is the mean GC mass (2.4×10^5 $\mathrm{M}_\odot$), and the numerical factor c is the luminosity corresponding to $M_\lambda = -15.0$ in solar luminosity units.

Adopting the specific frequencies derived in Section 7, the mass to luminosity ratios discussed in the previous section, with $c = 1.55 \times 10^8$ for the blue band, yield $\eta_{\mathrm{RGC}} = 1.25 \times 10^{-3}$ and $\eta_{\mathrm{BGC}} = 7.60 \times 10^{-3}$.

In addition, and following McLaughlin 1999, this definition can be revised in terms of the total baryonic mass, i.e. including the mass of hot gas. In this case we define a shell with inner and outer (spatial) radii of 11 and 66 Kpc, respectively. The adoption of the inner boundary attempts to decrease the effect of gravitational disruption on the GC sample while the outer one is the limit of our brightness profile. About 1800 red GCs and 1500 blue GCs fall within these boundaries that enclose 3.54×10^{11} and 0.55×10^{11} $\mathrm{M}_\odot$ of stars of the red and blue populations, respectively. On the other hand, adopting the X-ray analysis by Jones et al. (1997) and correcting their adopted distance (24 Mpc) to ours, we obtain a hot gas mass of 0.28×10^{11} $\mathrm{M}_\odot$. These quantities lead to an overall efficiency $\eta = 1.8 \times 10^{-3}$ for both GC populations combined. This value is somewhat smaller, but compares well, with the GC formation efficiency (2.9×10^{-3}) derived by McLaughlin (1999).

11 A COMPARISON BETWEEN GLOBULAR CLUSTERS, STARS, HOT GAS AND DARK MATTER DISTRIBUTIONS

11.1 Red GCs and total galaxy mass

The results presented in the previous sections are consistent with the existence of a link between the red GC and the (red and dominant) halo stellar population of NGC 1399. This connection is also supported by the GC kinematic behaviour. For example, Saglia et al. (2000) give a radial velocity dispersion for the halo stars of about 280 km s^{-1} (at 120 arcsec from the centre) in good agreement with the RGC value of 265 km s^{-1} (from R2004 data, without the velocity cut-off adopted by these authors). Taking into account that the derived volumetric profile for these clusters is consistent with a logarithmic spatial density derivative ($\mathrm{d}\ln(\rho)/\mathrm{d}\ln r) = -2.9$ (at galactocentric radii larger than $\approx$100 arcsec), and using the Jeans equation for the spherical and isothermal case, the resulting total mass within 100 Kpc of galactocentric radius ranges from 4.4 to 4.8×10^{11} $\mathrm{M}_\odot$ (for an anisotropy parameter β from 1.0 to -0.5).

11.2 Blue GCs, hot gas and dark matter

The X-ray emission of the Fornax cluster has been the subject of several works (e.g. Ikebe et al. 1992; Serlemitsos et al. 1993). *ROSAT* observations have been discussed by Jones et al. (1997) who fit a

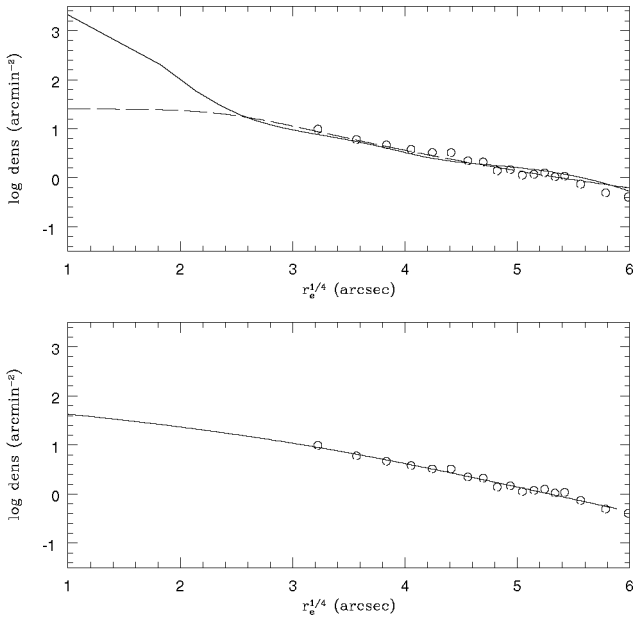

Figure 13. Upper panel: the NGC 1399 blue GCs density profile (open circles) compared with that of the hot X-ray emitting gas (continuous line: from Paolillo et al. 2002; dashed line: from Jones et al. 1997). Lower panel: blue GC compared with the (projected) dark matter profile obtained by R2004 using GC kinematics.

surface brightness profile of the form

$$S(r) = S(0)\left[1 + \left(\frac{r}{a}\right)^2\right]^{-3\beta+0.5} \quad (10)$$

centred on NGC 1399, obtaining best-fitting parameters $a = 45$ arcsec and $\beta = 0.35$. In turn, Paolillo et al. (2002) give a thorough description of the complex X-ray emission and suggest a composite beta model (including 'central', 'galaxy' and 'cluster' components). Both the Jones et al. (1997) and the Paolillo et al. (2002) profiles are depicted in Fig. 13 (upper panel) and exhibit a high level of coincidence with the surface density of the blue GC.

The lower panel in Fig. 13 shows the projected profile that gives a representation of the dark matter distribution (also shifted in ordinates) derived by R2004 on the basis of their GC kinematic study. These last authors note that a NFW profile (i.e. $\zeta = 1.0$; Navarro, Frenk & White 1996, 1997) with a scalelength $r_s = 394$ arccsec gives a good representation of the inferred volumetric density of dark matter. We remark that, although their fit covers a galactocentric range from approximately 2 to 8 arcmin ($r_e{}^{1/4}$ from 3.31 to 4.68), the profile extrapolation holds up to 20 arcmin (i.e. the approximate limit of the D2003 data). For this reason, and among all the acceptable sets of $\zeta - r_s$ values, we adopted $\zeta = 1.0$ and $r_s = 375$ arcsec as adequate for the BGC noting that our scalelength can be considered as identical (to within the uncertainties) with the value given in R2004.

As discussed in Section 6, volumetric profiles with different values of the ζ parameter can yield almost equivalent fits to the observed areal densities for galactocentric radii larger than 2 arcmin. This means that, beyond the very good agreement between the distribution of the blue GC and dark matter, the data do not allow us to support unambiguously that an NFW profile also holds in the inner regions of the galaxy. However, all these profiles are consistent with an spatial derivative $\mathrm{d}\ln(\rho)/\mathrm{d}\ln(r) \approx -1.4$ from 100 arcsec and outwards in galactocentric radius. If this value is adopted as representaive for the hot gas (according to Fig. 13) and for a temperature range of 1.1–1.4 KeV (Jones et al. 1997; Paolillo et al. 2002), the total gravitating mass within 100 Kpc assuming hydrostatic gas equilibrium, becomes 5.3–5.8 $\times 10^{11}$ $M_\odot$, i.e. comparable with that derived from the RGC kinematics mentioned before.

The fact that the slope of the density profiles of the blue GC and that corresponding to the X-ray emission associated with NGC 1399 seem similar was already suggested by Hilker et al. (1999). In turn, the similarity between the distribution of the blue GC and that of dark matter was also pointed out by Côté, Marzke & West (1998) in their analysis of the *outer* regions of the M87 GCS.

12 DISCUSSION

The surface brightness profiles presented in Section 4 cannot be matched with a single $r^{1/4}$ law, a feature already noted in previous works (e.g. Schombert 1986) that have also pointed out the presence of an outer corona that would entitle the classification of NGC 1399 as a cD galaxy (but see the difficulties inherent to such a classification described in R2004).

If in fact the formation of a given GC family occurs concomitantly with that of a diffuse stellar population that shares its age and chemical abundance, it may be expected that, after gravitational relaxation, both stars and clusters will exhibit similar spatial distributions. Although dynamical friction might play a differential role that remains to be estimated, globulars could be identified as tracers of both the spatial distribution and of the kinematic behaviour of coeval diffuse stellar populations. Then, the galaxy brightness profile would be the result of the 'luminosity weighted' composition of those events. This approach gives a proper fit of the NGC 1399 profile shape by assuming the presence of two dominant populations (although they might exhibit their own degree of internal inhomogeneity in terms of age and chemical abundance) typified by very different intrinsic specific frequencies S_n. As the blue stellar population becomes more prominent outwards, owing to its shallower areal density slope, the degree of 'cDness' of the galaxy can also be identified as a result of that population.

An important result of the analysis is that, even though both the red and the blue GC families do not exhibit a detectable change of their modal colours over a galactocentric range close to 100 Kpc, the composition of their associated diffuse stellar populations do lead to a blueward colour gradient that compares well with the observations.

A caveat remains, however, in the sense that the galaxy profile can be matched by adopting a stellar population density profile similar to that of the red GC and forcing a spatial colour gradient. This would imply, on the one hand, that for some reason the stellar and red GC enrichments were decoupled and, on the other, that blue GC formed in a process unable to form non-clustered stars.

Although the overall GC formation efficiency obtained in previous sections seems comparable to other values available in the literature (e.g. McLaughlin 1999) the considerably higher intrinsic S_n value of the blue population in comparison with the red one also implies a higher globular formation efficiency that may be indicative of a distinct formation environment. Possible explanations of this situation have been given in the literature in connection with the role of re-ionization as responsible of the termination of the star forming process or in the frame of the Searle & Zinn (1978) scenario. In this last case, relatively small gas clumps associated with the formation of the BGC are disrupted by supernovae.

As noted before, the profile fit does not give an acceptable description of the inner 30 arcsec in galactocentric radius where the galaxy is brighter and redder than predicted. This situation may arise from

the use of an inappropriate analytical profile, and/or the effect of GC disruption by gravitational forces (see, for example, Vesperini et al. 2003). Aperture integrated ($C - T_1$) colours measured by Ostrov et al. (1998) are indicative of the presence of a high-metallicity stellar population (Pickles 1985; Kuntschner 2000). This situation has similarities with other galaxies (e.g. the MW; McWilliam & Rich 1994) where bulge stars seem to have metallicities somewhat higher than those of the RGC. A distinctive kinematic behaviour of the NGC 1399 central region can be seen in the velocity dispersion profile obtained by Saglia et al. (2000). These facts indicate that the galaxy nucleus may have harboured a different sequence of stellar formation events disparate from those observed over much larger spatial scalelengths.

13 CONCLUSIONS: A TENTATIVE SCENARIO

Previous sections have described a possible approach to the link between GCs and the diffuse stellar population in NGC 1399 on a purely photometric basis. Although spectroscopic results (Forbes et al. 2001) indicate the existence of an age spectrum among its GC (and, presumably, in the associated diffuse stellar populations), the analysis of a significant volume of spectroscopic data in terms of age and metallicity is still missing.

In a cautious way, however, the results presented in the previous sections, and available in the literature, can be ordered into a working scenario that attempts to delineate a temporal sequence of events that might end in the observed situation, namely.

(i) The blue GC in NGC 1399 exhibits modal integrated colours that are comparable to those observed in other galaxies and are consistent with a frequently mentioned fact – the relative homogeneity of the blue GC population from one system to another, suggesting that their origin might have occurred before the formation of the dominant stellar population of the galaxy haloes. However, recent works (Lotz, Miller & Ferguson 2004; Strader, Brodie & Forbes 2004) indicate that a correlation between the integrated BGC colours and the galaxy absolute magnitude may exist. These results imply that, even though the BGC might have formed in a very early stage, these clusters 'knew' about the galaxy they were forming in.

(ii) There is a remarkable coincidence of the spatial distribution of the blue GC with that inferred for dark matter by R2004 on the basis of their kinematic study. We stress that, even though these last authors perform their analysis in a galactocentric range from 2 to 8 arcmin, the extrapolation of their dark mass profile (projected on the sky) matches that of the BGCs up to 20 arcmin (the outer limit in D2003 and in our analysis).

(iii) X-ray emitting hot gas, usually assumed to be at the virial temperature of galaxy clusters, also show a spatial distribution that, within the uncertainties, is coincident with that of the blue GC. We note that the mean metallicity of this gas ([Fe/H] $= -0.4$; Jones et al. 1997) is comparable to that of the RGC.

(iv) A revision of the R2004 kinematic data suggests that at least the outer blue GC in NGC 1399 may exhibit, as in other galaxies, a detectable amount of 'solid-body'-like rotation. The presence of angular momentum in these clusters has been noted, for example, in M87 (Kissler-Patig & Gebhardt 1998) and NGC 4472 (Côté et al. 2003).

All these features strongly suggest that blue GC may have had their origin at a very early phase of stellar formation, sharing the evolution of dark matter clumps in the non-dissipative collapse that finally formed the most massive component of galaxy haloes, a fact that might also be reflected by their high radial velocity dispersion. In this context, the usefulness of simple closed box-type chemical evolution models has been noted, for example, by Harris & Harris (2000), Durrell, Harris & Pritchet (2001) and, in the particular case of the MW, by VanDalfsen & Harris (2004). Along these lines, the scenario described by Harris & Harris (2002) for NGC 5128, where early star formation goes on with an initial stage of rapid infall of metal-poor gas, and based on the similarities with NGC 1399 noted in Section 9, may also seem relevant for this last galaxy.

In turn, red GC seem connected with the formation of the dominant stellar population, probably at the expense of gas that has suffered a rather inhomogeneous dissipative collapse leading to angular momentum loss and to their broad chemical abundance distribution. This process might have been boosted by the effect of the very early enrichment provided by the blue GC (and the associated diffuse stellar population).

The idea that GC may have played a role as early 'seeds' of chemical enrichment was already put forward by De Young, Lind & Strom (1983). The main problem with their model is that the small mass locked in GC could not provide enough heavy elements to increase the overall metallicity level. This problem is overcome if, in fact, most of the enrichment comes not from the cluster themselves but from a much more massive (although less conspicuous) diffuse stellar population. The role of the oldest GC and its associated stellar population in the re-ionization of the Universe would also be enhanced on the same argument.

As a reference, we note that such a blue stellar population might provide some 1.9×10^9 $M_\odot$ of heavy elements within a galactocentric radius of 100 Kpc. This mass of heavy elements arises in an estimated stellar mass of 8.1×10^{10} $M_\odot$ contained in the blue population (from the blue stellar light profile and the (M/L) ratios given in Section 9) and adopting the net yields ($\eta = 0.023$) given by Portinari, Chiosi & Bressan (1998) and revised by Cora (in preparation) for a very low metallicity population. If the current red stellar population (8.1×10^{10} $M_\odot$) was mostly in gaseous form at that stage, the injected heavy metals would have raised the chemical abundance to about 0.15 $Z_\odot$.

This enrichment is about one third of the mean abundance of the red stellar population (inferred from the associated RGC), i.e not enough to explain the observed differences between both populations. However, that level of enrichment might have had an important impact on the gas cooling function, improving the star formation efficiency and triggering the process that ended up with the broad abundance distribution of the red stellar population (and also on the current chemical composition of the hot gas).

The much higher formation efficiency of the blue clusters suggest very different environmental conditions from those that prevailed for the red globulars. This fact, and the impact of a diffuse and low-metallicity stellar population on the subsequent process of galaxy formation remains worthy of exploration.

A final comment about the possible existence of such a stellar population around NGC 1399 deals with the fact that, being that galaxy in the neighbourhood of the Fornax cluster barycenter, it is not clear if the association is with this galaxy or with the cluster as a whole. For example, Bassino et al. (2003) argue that GC, apparently not associated with galaxies in the field, can be identified at angular distances as large as 4800 arcsec from NGC 1399 (a distance comparable to the galaxy virial radius); the eventually associated diffuse population at that radius would be hard to detect as the expected blue surface brightness would be in the range of 31–32 mag arcsec^{-2}.

ACKNOWLEDGMENTS

The authors are grateful to Dr Juergen Scheer for allowing the use of his data. One of us (FF) carried out this work with a Research Fellowship from CONICET. This work was funded with grants from CONICET, ANPCYT and Universidad Nac. de La Plata (Argentina).

REFERENCES

Ashman K. M., Conti A., Zepf S. E., 1995, AJ, 110, 1164
Bassino L., Cellone S. A., Forte J. C., Dirsch B., 2003, A&A, 399, 489
Baugh C. M., Cole S., Frenk C. S., Lacey C. G., 1998, ApJ, 498, 504
Beasley M. A., Baugh C. M., Forbes D., Sharples R. M., Frenk C. S., 2002, MNRAS, 347, 1150
Binney J., Tremaine S., 1987, in Galactic Dynamics, Princeton Univ. Press
Canterna R. 1976, AJ, 81, 228
Caon N., Capaccioli M., Donofrio M., 1994, A&AS, 106, 199
Capuzzo-Dolcetta R., Donnarumma I., 2001, MNRAS, 328, 645
Capuzzo-Dolcetta R., Tesseri A., 1999, MNRAS, 308, 961
Côté P., Marzke R. O., West M. J., 1998, ApJ, 501, 554
Côté P., McLaughlin D. E., Cohen J. G., Blakeslee J. P., 2003, ApJ, 591, 850
De Young D. S., Lind K., Strom S. E., 1983, PASP, 95, 401
Dirsch B., Richtler T., Geisler D., Bassino L. P., Gieren W. P., 2003, AJ, 125, 1908 (D2003)
Durrelll P. R., Harris E. W., Pritchet C. J., 2001, AJ, 121, 2557
Eggen O., Lynden Bell D., Sandage A., 1962, ApJ, 136, 748
Forbes D. A., Forte J. C., 2001, MNRAS, 322, 257
Forbes D. A., Brodie J. P., Huchra J., 1997, AJ, 113, 887
Forbes D. A., Brodie J. P., Grillmair C. J., 1998, MNRAS, 293, 325
Forbes D. A., Beasley M. A., Brodie J. P., Kissler-Patig M., 2001, ApJ, 563, 143
Forte J. C., Strom S. E., Strom K., 1981, ApJ, 245, L9
Forte J. C., Geisler D., Kim E., Lee M. G., Ostrov P. G., 2002, in Geisler D., Grebel E. K., Minniti D., eds, Proc. IAU Symp. 207, Extragalactic Star Clusters. Astron. Soc. Pac., San Francisco, p. 251
Geisler D., 1996, AJ, 111, 480
Geisler D., Forte J. C., 1990, ApJ, 350, L5
Geisler D., Lee M. G., Kim E., 1996, AJ, 111, 1529
Grillmair C. J., Forbes D. A., Brodie J. P., Elson R. A. W., 1999, AJ, 117, 167
Harris G. L. H., Harris W. E., 2000, AJ, 120, 2423
Harris H., Canterna R., 1977, AJ, 82, 798
Harris W. E., 1996, AJ, 112, 1487
Harris W. E., 2003, in Kissler-Patig M., ed., Extragalactic Globular Cluster Systems. Springer, Berlin, p. 317
Harris W. E., Harris G. L. H., 2002, AJ, 123, 3108
Harris W. E., van den Bergh S., 1981, AJ, 86, 1627
Harris W. E., Harris G. L. H., McLaughlin D. E., 1998, AJ, 115, 1801
Hilker M., Infante L., Richtler T., 1999, A&AS, 138, 55
Ikebe Y. et al., 1992, ApJ, 384, L5
Jones C., Stern C., Forman W., Breen J., David L., Tucker W., 1997, ApJ, 482, 143
Killeen N. E. B., Bicknell G. V., 1988, ApJ, 325, 165
Kissler-Patig M., 2002, in Geisler D., Grebel E. K., Minniti D., eds, Proc. IAU Symp. 207, Extragalactic Star Clusters. Astron. Soc. Pac., San Francisco, p. 207
Kissler-Patig M., Gebhardt K., 1998, AJ, 116, 2237
Kundu A., Whitmore B. C., 1998, AJ, 116, 2841
Kuntschner H., 2000, MNRAS, 315, 184
Larsen S. S., Richtler T., 2000, A&A, 354, L836
Lee H.-C., Lee Y. W., Gibson B. K., 2002, AJ, 124, 2664
Lotz J. M., Miller B. W., Ferguson H. C., 2004, AJ, 613, 262
McLaughlin D. E., 1999, AJ, 117, 2398
McWilliam A., Rich R. M., 1994, ApJS, 91, 749
Michard R., 2000, A&A, 360, 85
Navarro J. F., Frenk C. S., White S. D. M., 1996, ApJ, 462, 563
Navarro J. F., Frenk C. S., White S. D. M., 1997, ApJ, 490, 493
Ostrov P. G., Geisler D., Forte J. C., 1993, AJ, 105, 1762
Ostrov P. G., Forte J. C., Geisler D., 1998, AJ, 116, 2854
Paolillo M., Fabbiano G., Peres G., Kim D.-W., 2002, ApJ, 565, 883
Peebles P. J. E., Dicke R. H., 1968, ApJ, 154, 891
Pickles A. J., 1985, ApJ, 296, 340
Portinari L., Chiosi C., Bressan A., 1998, A&A, 334, 505
Reed B. C., Hesser J. E., Shawl S. J., 1988, PASP, 100, 545
Richtler T. et al., 2004, AJ, 127, 2094 (R2004)
Ricotti M., 2002, MNRAS, 336, L33
Saglia R. P., Kronawitter A., Gerhard O., Bender R., 2000, AJ, 119, 153
Santos M. R., 2003, in Kissler-Patig M., ed., Extragalactic Globular Cluster Systems. Springer, Berlin, p. 348
Scheer J., 1987, Appl. Optics, 26, 3077
Schlegel D., Finkbeiner D., Davis M., 1998, ApJ, 500, 525
Schombert J. M., 1986, ApJS, 60, 603
Schweizer F., 1987, Nearby Normal Galaxies. From the Planck Time to the Present. Springer, New York, p. 18
Searle L., Zinn R., 1978, ApJ, 205, 357
Serlemitsos P., Loewenstein M., Mushotzky R., Marshall F., Petre R., 1993, ApJ, 413, 518
Strader J., Brodie J. P., Forbes D. A., 2004, AJ, 127, 3431
VanDalfsen M. L., Harris E. W., 2004, AJ, 127, 368
Vesperini E., Zepf S. E., Kundu A., Ashman K. M., 2003, ApJ, 593, 760
Worthey G., 1994, ApJS, 95, 107

This paper has been typeset from a TEX/LATEX file prepared by the author.